Comparative Analysis of a Floating Mooring Line-Driven Platform (FMDP) Having Different Mooring Lines Patterns

Mamon M. Horoub
Entrepreneurship Institute
King Fahd University of Petroleum and Minerals
Dhahran 31261, Saudi Arabia
e-mail: horoub@kfupm.edu.sa

Sikandar Khan
Deanship of Academic Development
King Fahd University of Petroleum and Minerals
Dhahran 31261, Saudi Arabia
e-mail: sikandarkhan@kfupm.edu.sa

Sajid Ali
Department of Mechanical Engineering
King Fahd University of Petroleum and Minerals
Dhahran 31261, Saudi Arabia
e-mail: sajidali@kfupm.edu.sa

Ayman M. Horoub
Mathematics Department
Hebron University, Hebron, Palestine
e-mail: hroub.math@gmail.com

***Abstract*—In this study, dynamic analysis is conducted on a Floating Mooring Line-Driven Platform (FMDP) subjected to sea wave forces. The effect of changing mooring lines pattern is investigated to enhance the dynamic behavior of the FMDP. The analysis is demonstrated with six mooring lines FMDP. A new mooring lines pattern (6-3-3) is studied and compared with the (6-6) Stewart-Gough manipulator pattern. The dynamic behavior, cables tension, and platform stiffness are determined across FMDP effective area. The dynamic analysis of FMDP is improved using the new mooring lines pattern (6-3-3).**

Keywords-dynamic analysis; effective area; floating mooring line-driven platform; sea waves; Stewart-Gough manipulator, 6-6 and 6-3-3 FMDP

I. INTRODUCTION

Mooring line parallel manipulators (MPM) are manipulators that are known for their large workspace and high acceleration capability. Cables are used instead of rigid-links, to move the moving structure of MPM. MPM are ideal for many applications such as handling of hazardous materials, disaster search and rescue efforts [1]. In addition to that, it is used in telescope radio stations, sports and entertainment fields. There have been a number of MPM designs presented in the literature such as NIST Robocrane [2], Falcon-7 [3], WARP [4], WiRo [5], DeltaBot [6], and the hybrid cable-actuated robot developed by Mroz and Notash [7].

Mooring line platforms are combination of two parts, a moving structure part and a mooring line system. Designing the mooring line system is important because it controls the moving structure part. There are several aspects which must be considered when designing a mooring line system, such as the mooring lines' material properties, mooring lines' lengths, mooring lines' weight, and cost effectiveness [8]. The mooring lines' pattern is another factor that could be considered. Few researchers studied the effect of mooring lines' pattern on the performance of the floating platforms [9]-[12]. On the other hand, several studies use mooring lines to analyze the workspace and the motion responses of MPMs [13]-[22]. MPMs can be used in marine environment for oil and gas exploration [23], [24].

Based on the study of the available literature on MPM, the effect of marine environment on the MPM is one of the aspects that has not been fully explored. Floating mooring line-driven platform (FMDP) performance is controlled by mooring lines' positions [25], [26]. Mooring lines' positions (i.e. mooring lines' pattern) can be used to enhance the FMDP performance and to reduce the chance of system failure (i.e. having negative cables' tensions). One of the solutions in FMDP pattern is changing the vertical elevation for some of the cable positions on the floating platform. Therefore, this work aims to study the effect of having two different patterns on the performance of FMDP. A new mooring lines pattern (6-3-3) will be studied and compared with the (6-6) Stewart-Gough manipulator pattern. The dynamic behavior, cables tension, and platform stiffness, will be determined across FMDP effective area (i.e. workspace).

The general layout of the floating cable-driven platform is shown in Fig. 1. It consists of six mooring lines driven by motors/reels mounted on the floating structure of the FMDP. It consists of mooring lines arranged in a form similar to the6-6 Stewart Gough parallel robot, depicted in Fig. 2.

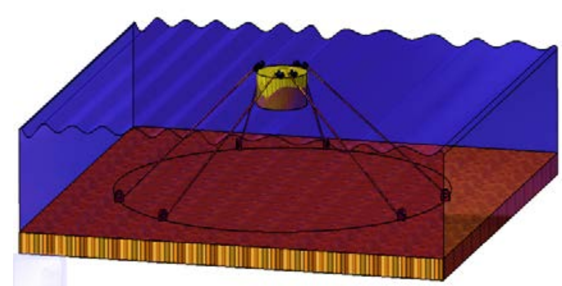

Figure 1. General floating cable-driven platform.

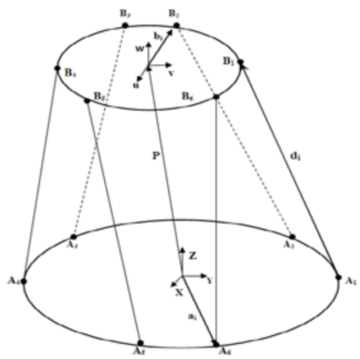

Figure 2. 6-6 Stewart Gough platform.

II. WAVE FORCES

The Floating mooring line-driven platform (FMDP) is subjected to dynamic forces from the sea waves caused by external climatic factors. To determine the effect of the sea forces on the FMDP, the floating structure will be considered as a circular rigid body with a radius “a” and submerge depth “b” that can have three degree of freedom (i.e. surge and heave translation motions, and pitch rotational motion). Figure 3 shows the application of the water wave on the floating structure. It has amplitude of $H/2$, wavelength of λ and it moves along the positive x-axis. The coordinate frame of reference is located on still water level (SWL).

This study follows the work of Finnegan et al [27] in which the fluid domain was divided into two regions: an interior region under the cylinder (marked as 1 in Figure 3) and an exterior region (marked as 2 in Fig. 3). Based on solving the scattering and radiation problem, the analytical solution of the water wave excitation forces on a circular floating structure was given as [27]:

$$\hat{F}_x = -\frac{\pi i \rho_f g H a}{k_o}\left(\mathrm{J}_1(k_o a) - \frac{\mathrm{J}_1'(k_o a)}{\mathrm{H}_1'(k_o a)}\mathrm{H}_1(k_o a)\right)(1 - \mathrm{e}^{-k_o b}) \qquad (1)$$

$$\hat{F}_z = -2\pi i \rho_f \omega a \sqrt{\frac{2}{\pi}} \int_0^\infty \mathrm{P}_0(\xi)\frac{\mathrm{I}_1(\xi r)}{\xi \mathrm{I}_0(\xi a)} d\xi \qquad (2)$$

$$\hat{F}_T = T_y = -\pi i \rho_f g H a \left(\mathrm{J}_1(k_o a) - \frac{\mathrm{J}_1'(k_o a)}{\mathrm{H}_1'(k_o a)}\mathrm{H}_1(k_o a)\right) * \int_0^b (z-b) e^{-k_o z}\, dz - \pi i \rho_f \omega a^2 \sqrt{\frac{2}{\pi}} \int_0^\infty \mathrm{P}_1(\xi)\frac{\mathrm{I}_2(\xi r)}{\xi \mathrm{I}_1(\xi a)} d\xi \qquad (3)$$

$$F_j = \hat{F}_j\, \mathrm{e}^{-i\omega t}\ , \quad j = x, z \text{ and } T \qquad (4)$$

where J_m denotes a Bessel functionof the first kind of order m, I_m denotes a modified Bessel function of the first kind of order m, H_m is the Hankel function of the first kind of order m, primes denote differentiation with respect to argument; ω is the water wave frequency, k_0 is the wavenumber, $k_0 = 2\pi/\lambda$, λ is the wavelength, H is the wave height, ϵ_m is Neumann's number, $\epsilon_o = 1$, $\epsilon_m = 2$, $m \geq 1$, and $\mathrm{P_m}(\xi) = -\frac{gH}{2\omega}\epsilon_m i^{m+1}\sqrt{\frac{2}{\pi}}\left(\mathrm{J_m}(k_o a) - \frac{\mathrm{J_m'}(k_o a)}{\mathrm{H_m'}(k_o a)}\mathrm{H}_m(k_o a)\right)\frac{\mathrm{e}^{-k_o b} k_o}{\xi^2 + k_o^2}$.

Fig. 4 shows the wave forces using the values mentioned in Table I.

TABLE I. VALUES ARE USED IN THE SIMULATIONS

Parameters	a (m)	d (m)	k_o (m^{-1})	H (m)	ρ_f $(\frac{kg}{m^3})$	b_w (m)	g $(\frac{kg}{m^3})$
Values	5	50	0.16095	1	1000	0.5	9.81

where b_w is the submerge depth due to weight.

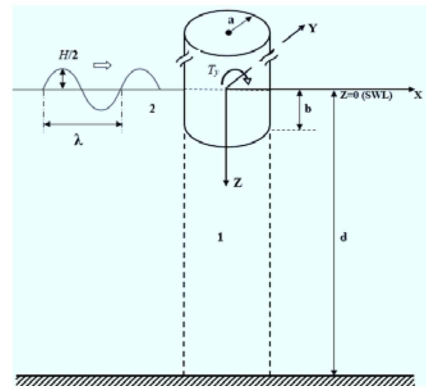

Figure 3. Water wave subjected to a floating structure.

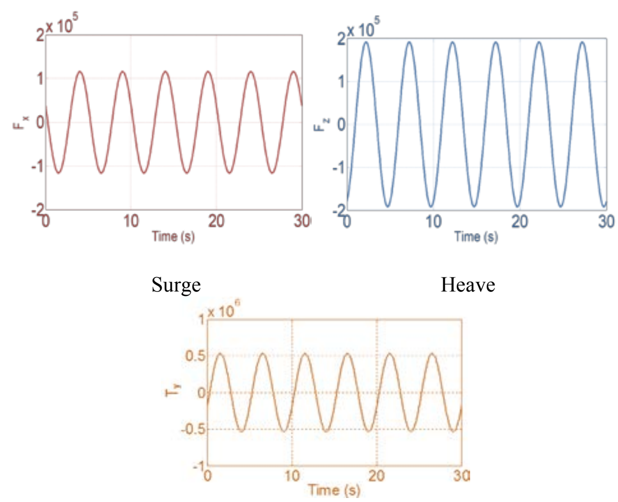

Figure 4. Surge, heave, and pitch excitation forces.

III. DYNAMIC ANALYSIS

In this section modal analysis technique is used in the dynamic analysis of the floating mooring line-driven platform (FMDP). Following the work of Behzadipour and Khajepour [22], the stiffness matrix of the platform is expressed as:

$$\mathbf{K} = \frac{\mathbf{dF}}{\mathrm{dp}} = \mathbf{K}_k + \mathbf{K}_\tau \qquad (5)$$

$$\mathbf{K}_k = \sum_{i=1}^{6} k_i \begin{bmatrix} \hat{s}_i \hat{s}_i^T & \hat{s}_i \hat{s}_i^T [b_i \mathrm{X}]^T \\ [b_i \mathrm{X}]\hat{s}_i \hat{s}_i^T & [b_i \mathrm{X}]\hat{s}_i \hat{s}_i^T [b_i \mathrm{X}]^T \end{bmatrix} \qquad (6)$$

$$\mathbf{K}_\tau = \sum_{i=1}^{6} \frac{T_i}{d_i} \begin{bmatrix} \mathrm{I} - \hat{s}_i \hat{s}_i^T & (\mathrm{I} - \hat{s}_i \hat{s}_i^T)[b_i \mathrm{X}]^T \\ [b_i \mathrm{X}](\mathrm{I} - \hat{s}_i \hat{s}_i^T) & [b_i \mathrm{X}](\mathrm{I} - \hat{s}_i \hat{s}_i^T)[b_i \mathrm{X}]^T - d_i[\hat{s}_i \mathrm{X}][b_i \mathrm{X}] \end{bmatrix} \qquad (7)$$

where $P = [\,p_x \quad p_y \quad p_z \quad \theta_x \quad \theta_y \quad \theta_z\,]^T$ is a position vector of the moving structure with respect to the XYZ fixed frame, showed in Figure 2 ; k_i is the i_{th} cable stiffness; **I** is the identity matrix; $\hat{s}_i$ is the unit vector along the cable direction; $\mathbf{K}_k$ is the stiffness matrix of the FMDP as a result of the cable stiffness; $\mathbf{K}_\tau$ is the FMDP stiffness matrix as a result of the cable tensions; and $[\hat{s}_i X]$ and $[b_i X]$ are matrices representing the cross product operators as:

$$[\hat{s}_i X] = \begin{bmatrix} 0 & -\hat{s}_{iz} & \hat{s}_{iy} \\ \hat{s}_{iz} & 0 & -\hat{s}_{ix} \\ -\hat{s}_{iy} & \hat{s}_{ix} & 0 \end{bmatrix},\ [b_i X] = \begin{bmatrix} 0 & -b_{iz} & b_{iy} \\ b_{iz} & 0 & -b_{ix} \\ -b_{iy} & b_{ix} & 0 \end{bmatrix} \quad (8)$$

It is not beneficial to rely on the term values in **K** because the translational and the rotational stiffness values in **K** cannot be compared with each other due to the difference in the physical units. Instead, we will use the natural frequencies of the FMDP to meaningfully evaluate its stiffness. The natural frequencies have common physical units (Hz) and are indicative of the FMDP stiffness. Considering the cables as springs, the natural frequencies of the FMDP are calculated as [25], [26], and [28].

$$f_j^k = \frac{\sqrt{eig_j\left(\mathbf{M}^{-1}\mathbf{K}^k\right)}}{2\pi} \quad (9)$$

where f_j^k is the jth natural frequency of the FMDP at the kth pose (in Hz); $eig_j\,(matrix)$ is the jth eigen value of the matrix; $\mathbf{M}^k$ is the stiffness matrix of the FMDP at the kth pose; **M** is the principal inertia matrix of FMDP.
Equation (10) represents the FMDP system which the surge, heave, and Pitch DOFs are considered. **K** is the stiffness, **M** is the mass matrix and **f** is the forces.

$$\mathbf{M}\ddot{\mathbf{x}} + \mathbf{K}\mathbf{x} = \mathbf{F} \quad (10)$$

where $\mathbf{F} = [\,F_x \quad (F_z + F_b) \quad T_y\,]^{\mathrm{T}}$, F_b is the buoyancy force.
Depending on the modal analysis method, Equation (10) can be converted to uncoupled differential equations as follows:

$$\mathbf{x}_i(t) = \mathbf{U}\mathbf{q}_i(t) \quad (11)$$

$$\mathbf{MU}\ddot{\mathbf{q}} + \mathbf{KU}\mathbf{q} = \mathbf{f} \quad (12)$$

$$\mathbf{U}^T\mathbf{MU}\ddot{\mathbf{q}} + \mathbf{U}^T\mathbf{KU}\mathbf{q} = \mathbf{U}^T\mathbf{f} \quad (13)$$

$$\ddot{\mathbf{q}}_i(t) + \omega_i^2\mathbf{q}_i(t) = \mathbf{n}_i(t) \quad (14)$$

$$\mathbf{n}_i(t) = \mathbf{U}^T\mathbf{f} \quad (15)$$

where the $\mathbf{x}_i(t)$ are the generalized coordinates, $\mathbf{q}_i(t)$ are the natural coordinates, ω_i are the natural frequencies of the system, **U** is the modal matrix (shape vectors) and $i = 1, 2$ and 3.

$$\mathbf{q}_i(t) = \frac{1}{\omega_i}\int_0^t \mathbf{n}_i(\tau)\sin\omega_i(t-\tau)\,d\tau\,, i = 1,2 \text{ and } 3 \quad (16)$$

Equation (16) represents the solution of Equation (14) where $\mathbf{x}_i(t) = \mathbf{U}\mathbf{q}_i(t)$.

To avoid mooring line slack, it is required to have a positive mooring line's tension in the FMDP. Equation 17 represents how to calculate the mooring lines' tensions,

$$\mathbf{T}_i = k\Delta L i = 1, \ldots, 6 \quad (17)$$

where **T** is the cable tensions, k is the mooring line stiffness, and ΔL is the change in mooring line length. The platform positive tensions were maintained by varying the submerged depth of the platform.

IV. Modification Analysis

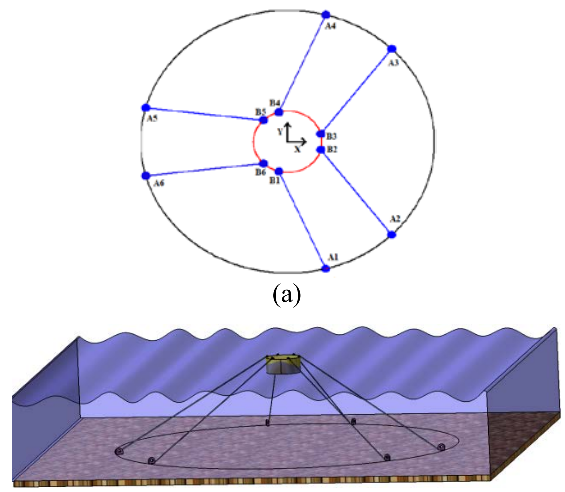

(a)

(b)

Figure 5. 6-6 FMDP configuration (a) 2D (b) 3D.

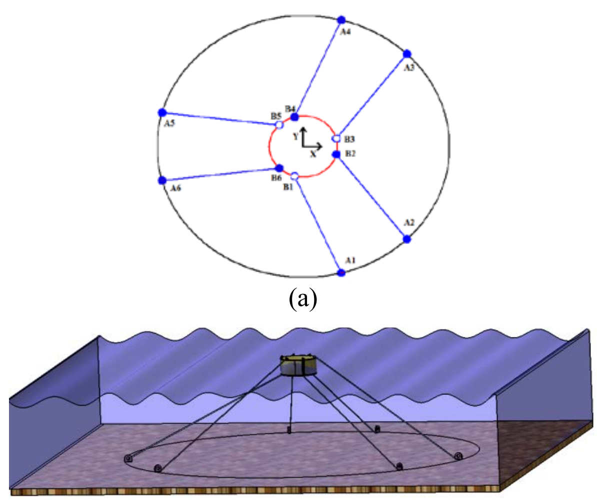

(a)

(b)

Figure 6. 6-3-3 FMDP configuration (a) 2D (b) 3D.

The layout of the floating mooring line-driven platform (FMDP) is shown in Fig. 5. The six cables are connected with the anchors which are located, with respect to negative Y axis, at points $A_1, A_2, A_3, A_4, A_5,$ and A_6 at angles $15, 45, 135, 165, 255,$ and 285 degrees, respectively, around the perimeter of the base circle (with 200 m radius) on the sea bed. Also, these six cables are driven by six motors on the top surface of the platform (circular disc with 5 m radius), located with respect to negative Y axis, at points $B_1, B_2, B_3, B_4, B_5,$ and B_6 at angles $345, 75, 105, 195, 225,$ and 315 respectively. The distance between the base and the platform is 50 m, which is the assumed water depth.

The new configuration (6-3-3 FMDP) is shown in Fig. 6. While three cables' positions (B_1, B_3, B_5) are connected to the bottom surface edge of the floating structure of FMDP, the remaining (B_2, B_4, B_6) are fixed to the top surface edge of the floating structure of FMDP.

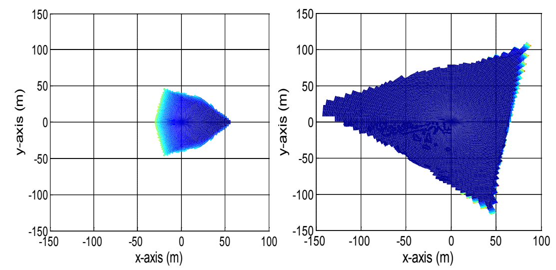

(a) (b)

Figure 7. Workspace of the FMDP using Table I data (a) 6-6 configuration (b) 6-3-3 configuration.

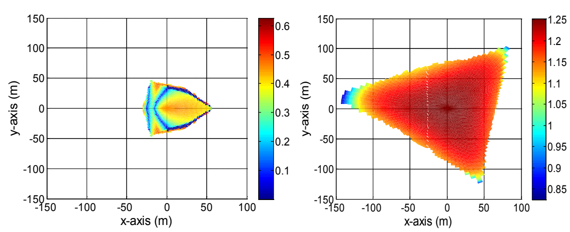

(a) (b)

Figure 8. Minimum Frequency (color, Hz) in the workspace shown in Fig. 7 (a) 6-6 configuration (b) 6-3-3 configuration.

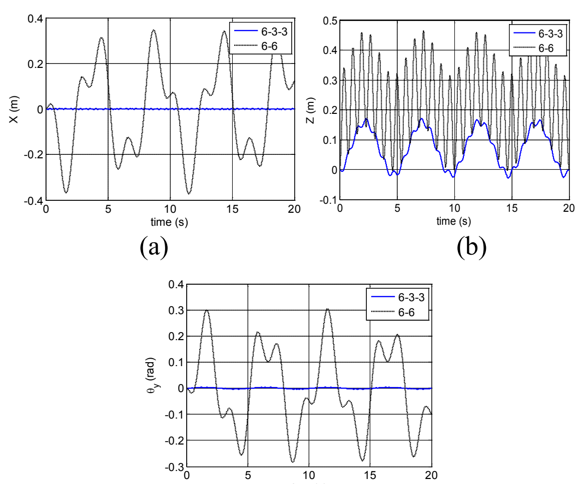

(c)

Figure 9. 6-3-3, and 6-6 FMDP dynamical responses (a) surge (b) heave (c) pitch.

The workspace for the 6-6 and 6-3-3FMDP configuration is shown in Fig. 7. It showed the sea surface area in which the floating structure of FMDP can operate without losing its cables' tensions. It is obvious that the 6-3-3 FMDP workspace is larger than the 6-6 FMDP workspace.

Fig. 8 showed the minimum natural frequency, within the same workspace in Figure 8, for 6-6 and 6-3-3 FMDPs. The 6-3-3 FMDP has higher minimum natural frequency in all FMDP poses. So, it is evident that the stiffness of 6-3-3 FMDP is much higher than the stiffness of 6-6 FMDP.

To compare between 6-6, and 6-3-3 FMDPs, dynamical study has been elaborated for the both platforms with the same submerged depth and in the same location where x=0m, and y=0 m. Fig. 9 represent the FMDP displacement when x = 0m,y = 0 m and b=1.28 m. It is clear that the response of 6-3-3 FMDP is much stable and better than 6-6 FMDP.

V. Conclusion

A marine application for floating mooring line-driven platform (FMDP) was proposed in this study, in which the moving platform operates in a certain workspace on the sea surface. The workspace, stiffness, displacement, and force equations for this platform were investigated. The dynamical analysis response has been calculated on the sea surface for a certain pose. This paper presented an analysis of a floating mooring line-driven platform consisting of a six cables and a solution to get larger workspace, higher stiffness, and better dynamics behavior for FMDP. The platform positive tensions were maintained by varying the submerged depth of the platform. The paper discussed briefly for 6-3-3 FMDP the value of the submerge depth for 6-3-3 FMDP that is needed in every pose to minimize the tensions generated in the cables. Finally, it can be concluded that the 6-3-3 FMDP is more stable and better in marine environment as compared to the 6-6 FMDP.

References

[1] P. H. Borgstrom, N. P. Borgstrom, M. J. Stealey, B. Jordan, G. Sukhatme, M. A. Batalin, and W. J. Kaiser, "Discrete trajectory control algorithms for nims3d, an autonomous under constrained three-dimensional cabled robot," In Intelligent Robots and Systems, 2007. IEEE/RSJ International Conference on, pp. 253-260, 2007.

[2] J. Albus, R. Bostelman, and N. Dagalakis, "The Nist Robocrane," J. Robotic Systems, vol. 10, no.5, pp. 709-724, 1993.

[3] S. Kawamura, W. Choe, S. Tanak, "Development of an Ultrahigh Speed Robot Falcon Using Wire Driven Systems," in Proc. IEEE Int. Conf. on Robot. Autom., pp. 215-220, 1995.

[4] K. Maeda, S. Tadokoro, T. Takamori, M. Hiller, and R. Verhoeven, "On Design of a Redundant Wire-driven Parallel Robot WARP Manipulator," in Proc. IEEE Int. Conf. on Robot. Autom., vol. 2, pp. 895-900.

[5] C. Ferraresi, M. Paoloni, and F. Pescarmona, "A new 6-dof Parallel Robotic Structure Actuated by Wires: The Wiro-6.3," J. of Robotic Systems, vol. 21, no. 11, pp. 581-595, 2004.

[6] S. Behzadipour, A. Khajepour, "A New Cable-based Parallel Robot with Three Degrees of Freedom," Multibody System Dynamics, vol. 13, pp. 371-383, 2005.

[7] G. Mroz, L. Notash, "Wire-actuated Robots with a Constraining Linkage," J. Robotic Systems, vol. 21, no. 12, pp. 677-678, 2004.

[8] S. A. R. d. S. Maffra, M. A. C. Pacheco, and I. F. M. de. Menezes, "Genetic Algorithm Optimization for Mooring Systems," generations, vol. 1, p. 3, 2003.

[9] M. Shafieefar and A. Rezvani, "Mooring optimization of floating platforms using a genetic algorithm," Ocean Engineering, vol. 34, pp. 1413-1421, 2007.

[10] B. Monteiro, C. Albrecht, and B. Jacob, "Application of the Particle Swarm Optimization Method on the Optimization of Mooring Systems for Offshore Oil Exploitation," in Procs. of the 2nd International Conference on Engineering Optimization, 2010.

[11] O. Montasir, A. Yenduri, and V. Kurian, "Effect of mooring line configurations on the dynamic responses of truss spar platforms," Ocean Engineering, vol. 96, pp. 161-172, 2015.

[12] I. Felix-Gonzalez and R. S. Mercier, "Optimized design of statically equivalent mooring systems," Ocean Engineering, vol. 111, pp. 384-397, 2016.

[13] S. Kawamura and K. Ito, "A New Type of Master Robot for Teleoperation Using a Radial Wire Drive System," in Proc. IEEE Int. Conf. Intell. Robots and Systems, pp. 55-60, 1993.

[14] A. Ming and T. Higuchi, "Study on Multiple Degree-of-Freedom Positioning Mechanism Using Wires (Part 1) ," Int. J. Japan Society of Precision Engineering, vol. 28, no. 2, pp. 131-138, 1994.

[15] R. G. Roberts, T. Graham, and T. Lippitt, "On the Inverse Kinematics, Statics, and Fault Tolerance of Cable-Suspended Robots," J. Robotic Systems, vol. 15, no. 10, pp. 581-597, 1998.

[16] J. Pusey, A. Fattah, S. Agrawal, and F. Messina, "Design and Workspace Analysis of a 6-6 Cable-suspended Parallel Robot," Mechanism and Machine Theory, vol. 39, pp. 761-778, 2004.

[17] E. Stump and V. Kumar, "Workspaces of Cable-Actuated Parallel Manipulators," ASME J. Mechanical Design, vol. 128. no. 1, pp. 159-167, 2006.

[18] C. B. Pham, S. H. Yeo, G. Yang, M. S. Kurbanhusen, and I.-M. Chen "Force-closure Workspace Analysis of Cable-driven Parallel Mechanisms," Mechanisms and Machine Theory, vol. 41, pp. 53-69, 2006.

[19] P. Bosscher, A.T. Riechel, and I. Ebert-Uphoff, "Wrench-feasible Workspace Generation for Cable-driven Robots," IEEE Trans. Robotics, vol. 22, no.5, pp. 890-902, 2006.

[20] M. Gouttefarde and C. M. Gosselin, "Analysis of the Wrench-closure Workspace of Planar Parallel Cable-driven Mechanisms," IEEE Trans. on Robotics, vol. 22, no. 3, pp. 434-445, 2006.

[21] X. Diao and O. Ma, "Force-closure Analysis of General 6-DOF Cable Manipulators," in Proc. IEEE/RSJ Int. Conf. Intell. Robots and Systems, San Diego, USA, pp. 3931-3936, 2007.

[22] S. Behzadipour and A. Khajepour, "Stiffness of Cable-based Parallel Manipulators with Application to Stability Analysis," Journal of Mechanical Design, Vol. 128 / 303, January 2006.

[23] A. Ghaffar and M. Hassan, "Study on Cable Based Parallel Manipulator Systems for Subsea Applications," In Proceedings of the 3rd International Conference on Mechanical Engineering and Mechatronics, No. 154, pp. 1-8, 2014.

[24] A. Ghaffar and M. Hassan, "Failure Analysis of Cable Based Parallel Manipulators," Applied Mechanics & Materials, 736, 2014.

[25] M. M. Horoub, M. Hassan, and M. A. Hawwa, "Workspace analysis of a Gough-Stewart type cable marine platform subjected to harmonic water waves," Mechanism and Machine Theory, 120, pp.314-325, 2018.

[26] M. M. Horoub and M. A. Hawwa, "Analysis of a Spar Platform with Various Mooring System Configurations Under the Influence of Water Waves," International Journal of Offshore and Polar Engineering, 27(03), pp.283-292, 2017.

[27] W. Finnegan, M. Meere, and J. Goggins. "The wave excitation forces on a truncated vertical cylinder in water of infinite depth," Journal of Fluids and Structures 40:201-213, 2013.

[28] M. Hassan and A. Khajepour, "Analysis of a Large-Workspace Cable-Actuated Manipulator for Warehousing Applications," ASME IDETC/CIE Conference, San Diego, California, USA, 2009.